Available online at www.sciencedirect.com
SCIENCE DIRECT
Polymer 46 (2005) 5149–5160
polymer
www.elsevier.com/locate/polymer

pH-responsive swelling behavior of poly(vinyl alcohol)/poly(acrylic acid) bi-component fibrous hydrogel membranes

Xing Jin, You-Lo Hsieh*

Fiber and Polymer Science, Textile and Clothing Department, University of California, 227 Everson Hall, Davis, CA 95616, USA

Received 18 February 2005; received in revised form 15 April 2005; accepted 19 April 2005

Abstract

The pH-responsive dimensional expansion and mass uptake of bi-component hydrogels in the form of fibrous membranes and films were reported. Fibrous membranes and monolithic films were prepared from aqueous mixture of poly(vinyl alcohol) and poly(acrylic acid) at 3.5 COOH/OH molar composition via electrospinning and solution cast, respectively, then cross-linked by heat-induced esterification. Both forms of hydrogels exhibited increasing swelling with increasing pH. For hydrogel fibrous membranes, planar expansion was immediate without the time lag observed on the films, and equilibrium thickness expansion and mass uptake took far longer than planar expansion. The dimensional expansion in the thickness direction was much higher than that in the planar directions for the fibrous membranes, while they were comparable for monolithic films. The peculiar asymmetric dimensional expansion of fibrous membrane is explicable with the asymmetric distribution of the fibers on the planar and thickness directions, which is formed during layer-by-layer collection process of electrospinning. The fibrous membranes distinguished themselves as being far stronger and faster in re-absorption in the swollen state than the cast-films.

Keywords: Hydrogel; Ultra-fine fiber; pH-responsive

1. Introduction

Smart gels are stimuli-responsive 3D polymer networks that swell or contract in response to changes in external stimuli, such as temperature, pH, ionic strength, light, electric–magnetic field, etc. [1]. Polyelectrolytes, sometimes referred as ionic polymers or ionomers, have ionizable side groups and can be cross-linked to form smart gels. In the non-ionized state, the swelling of these gels is determined by the elasticity of the polymer chains and the thermodynamics of polymer–solvent mixing, essentially the same as non-ionic polymer networks. Beyond certain pH thresholds, polyelectrolyte gels become ionized, creating additional driving forces for expansion [2]. Take the anionic polyelectrolyte, poly(acrylic acid) (PAA), as an example, the swelling at low pH is characteristic of non-ionized PAA. At pH above the pK_a of acrylic acid (4.25), the carboxylic acid groups on every other main-chain carbon are ionized to $–COO^-$ and protons. The ionization leads to electrostatic repulsion between $–COO^-$ groups and increased osmotic pressure inside the polymer matrix, causing further expansion of the 3D polymer network. Similar extra expansions can be observed for cationic polymer gels when environmental pH decreases below a critic value.

Nearly all pH-responsive polyelectrolytes also respond to electric stimulus, another trigger for practical applications. In an electrical field, the discrete volume phase transition of polyelectrolyte gels could be induced by stress exerted on the charged sites of polymer network [3]. There exists a critical stress, below which gel expands and above which it collapses. For gels connected to an electrode, the electric activation had also been attributed to the pH changes caused by the electrolysis of water, which generates H^+ at anode and OH^- at cathode, respectively [4,5]. This explanation treats pH variation as the true stimulus.

PAA is a principle commercial super-absorbent [6] and a prototypical pH-responsive polyelectrolyte. The inter-penetrating networks (IPNs) [7] and copolymers [8] containing acrylic acid have also been reported to exhibit thermo-, electro- and pH-responsive behavior. Among the many

* Corresponding author. Tel.: +1 530 752 0843.
E-mail address: ylhsieh@ucdavis.edu (Y.-L. Hsieh).

0032-3861/$ - see front matter © 2005 Elsevier Ltd. All rights reserved.
doi:10.1016/j.polymer.2005.04.066

potential applications, these gels have been particularly investigated as 'artificial muscles', since most living organs, except bones, hairs, and skin, have gel-like structures. Exploration of polymer gels as artificial muscles began with pH-modulation as stimulus [9], and later involved electrical activation [10,11]. The electro-activated length change was reported in the early 1960s in a pioneering work using PAA cross-linked with polyvalent alcohols [4,9] and with polyacrylonitrile containing acrylic acid groups [5]. More recent examples include the electro-activated contractile behavior of thermally cross-linked PVA/PAA (4/1 wt ratio) thin strips ($1.5\times5\times0.012$ cm^3) [10] and electro-activated bending of PVA/PAA IPNs [12].

In this work, the PVA/PAA fibrous membranes were prepared from electrospinning, and the swelling behavior of their gels were studied in various pH buffers and compared with those of monolithic films. The fibrous membranes were rendered water-insoluble by cross-linking via heat-induced esterification. This work can serve as a model study to guide the development of electro-activation assemblies of hydrogels in the form of fibrous membranes.

Electrospinning can generate fibers with a diameter of several tens to hundreds nanometer from many polymers and is a technique with renewed interest and development in the last decade [13]. The electrospun membranes containing ultra-fine fibers have many exciting properties absent in traditional fibers or films, especially the much higher specific surface and wider range of inter-fiber pore structures. Though the stimuli-responsive behavior of polymer gels have been reported extensively, to the best of our knowledge, our group is the first to create smart gels via electrospinning into fibrous membranes that exhibited temperature- and pH-responsive behavior [14,15].

Previous studies on swelling of polymer gels commonly reported the mass uptake of liquids due to the ease of measurement. For applications like artificial muscles, dimensional transform during swelling is of primary concern [4,5]. In this work, actual dimensional expansion during swelling was investigated, in addition to mass uptake, to provide further insight into the swelling process. Here we measured the linear deformation in the thickness as well as the planar directions in fibrous membranes, and compared the swelling between these two directions as well as with monolithic films of the same compositions. Special attention was paid to the initial swelling behavior before reaching equilibrium, which provides useful information about the response rate to the stimuli.

2. Experimental

2.1. Materials

Both polyvinyl alcohol (PVA) and polyacrylic acid (PAA) were from Aldrich and used without further purification. PVA was 88% hydrolyzed polyvinyl acetate and had a M_w of 124–186 kDa. PAA had a M_v of 450 kDa. Five aqueous buffers with pH values of 2, 4, 5, 7, and 10 were used for swelling measurements (Table 1).

2.2. Solution cast and electrospinning

Both monolithic films and fibrous membranes were prepared from solution containing 6 g PAA/PVA mixture per 100 ml distilled water. A 5/1 PAA/PVA mass ratio that corresponded to a 3.5 COOH/OH mole ratio was employed. PAA was dissolved in distilled water with constant stirring at room temperature. PVA was then gradually added in. The mixture was stirred at room temperature for 1 day to reach a homogeneous and translucent solution.

Monolithic films were obtained by solution cast in a Teflon-lined box and dried at 40 °C for at least 1 day then at 80 °C under vacuum for at least 12 h. Fibrous membranes were produced by electrospinning the mixture solution, which was put in a 5 ml plastic Eppendorf pipette tip capped with a smaller one. The inner diameter of the small tip nozzle was ~0.8 mm. A stainless steel electrode was immersed in solution and connected to a power supply (Gamma High Voltage Supply, ES 30-0.1P). Grounded counter electrode was connected to the Al foil collector that was placed ~23 cm from the tip nozzle. The fibers were collected at a voltage of 10 kV. About 1 ml of solution was consumed every hour.

2.3. Thermal cross-linking

To render these monolithic films and fibrous membranes insoluble in water, samples were heated under vacuum, so that cross-linking was induced by esterification between the PVA hydroxyl and PAA carboxylic groups. To select suitable heating conditions, the fibrous membranes were heated at 140 and 120 °C for 5 min [15], immersed in water for a day, then dried for observation by scanning electron microscope. Sample heated at 140 °C could retain their fibrous form, while the one heated at 120 °C lost integrity greatly. Therefore, heating temperatures near 140 °C were selected for this study. Two lengths of heating, i.e. 5 and 8 min, were used to vary the extent of cross-linking (Table 2). After most solvent was evaporated, when cast film was not sticky anymore and still flexible, it was cut into pieces of the final sample size. The cut pieces of cast film were placed in an Al-foil-folded box for heating. The fibrous membranes were detached from Al foil collector and sandwiched between two 11.5×16.5 cm^2 Teflon films and under an 18.3 g weight during heating. The thickness values after heating processes were 0.12–0.25 mm and 0.3–0.5 mm for film and fibrous membrane, respectively.

2.4. Swelling measurement

The swelling measurements were the same for monolithic films and fibrous membranes. Samples were

Table 1
Sources and contents of the aqueous buffers

pH	2	4	5	7	10
Source	EM science	VWR	EM science	EM science	VWR
Content	HCl and glycine	Potassium hydrogen phthalate	NaOH and potassium hydrogen phthalate	Na_2HPO_4 and KH_2PO_4	Na_2CO_3 and $NaHCO_3$

completely immersed in individual buffers with pH between 2 and 10. For thickness measurements, the samples measuring 3×3 mm^2 and weighing between 1 and 3 mg were immersed in 18 ml buffers. Mass uptake and planar dimensional changes were measured with samples 6×6 mm^2 and weighing between 6 and 12 mg, using 18 ml buffer for the mass and 6 ml for the planar dimension measurements.

The mass, planar and thickness swelling ratios were calculated as the ratios of the corresponding measured values of swollen gels to that of original dry samples, and denoted as S_w, S_p, and S_t, respectively. S_p was the average of the swelling ratios in the width and length directions. The corresponding equilibrium swelling ratios were denoted as $S_{w,e}$, $S_{p,e}$, $S_{t,e}$, respectively. The experimental error was ±0.1 for S_p and S_t, and ±0.6 for S_w.

The planar dimensions, i.e. width and length, of samples placed in a transparent flat-bottom vessel were read to the nearest 0.5 mm. For mass and thickness swelling measurements, sample was removed from the buffer at certain time, and surface liquid was wiped off with tissue paper before measurement. Sample masses were weighed to the nearest 3 mg. The thickness values of the dry and hydrated gel were measured to the nearest 0.01 mm using a micrometer and a thermomechanical analyzer (Shimadzu TMA-60), respectively. For thickness measurements, each gel was sandwiched between two 11×11 mm^2 microscope cover glass with TMA probe on top exerting 3 g force. This provided the minimum force to keep the gel samples flat. Most of the experiments were taken at least twice to make sure they are reproducible.

3. Results and discussions

PAA is readily soluble in water. Previous work showed that PAA powder heated at 155 °C for 43 h remained soluble in dimethyl formamide and in dimethyl sulfoxide [17]. Extensive infrared studies have found that heating pure PAA below 170 °C led mainly to intra-chain anhydride formation from dehydration between carboxylic acid groups [16,17]. Inter-chain anhydride formation was observed only with heating above 170 °C [18] Adding cross-linkers was deemed necessary if heating below 170 °C is desired. PVA was, therefore, added to promote inter-molecular cross-linking via heat induced esterification between PVA hydroxyl and PAA carboxylic groups. The bi-component PVA/PAA samples in this work were heated for 5 and 8 min. These heating times were sufficient to render both films and fibrous membranes insoluble in aqueous solutions, and yet were much shorter than the commonly reported (45 min; 130 °C) [10]. All equilibrium swellings remained essentially unchanged for at least 2 days, indicating rather stable gel network structure in samples. Following an extended immersion in water, i.e. 2 weeks, greater extents of weight losses were observed on samples heated at a lower temperature or for a shorter time (Table 2). Assuming the reverse relationship between this measure of dissolution and cross-linking, the extents of cross-linking are CF-1 > CF-2 and ES-1 ≈ ES-3 > ES-2. This conclusion is further corroborated with the swelling data discussed below.

3.1. Monolithic film

The swelling patterns of two films thermally cross-linked at 137 and 143 °C for 8 min were similar (Figs. 1 and 2). Generally, the equilibrium swelling was reached between 5 and 60 min. The films thickened (Figs. 1(b) and 2(b)) and took up liquids (Figs. 1(c) and 2(c)) within the first minute upon exposure, however, showed little or no planar expansion (Figs. 1(a) and 2(a)) during the same time. The $S_{p,e}$ and $S_{t,e}$ are comparable at both the high (pH 10) and low pH (pH 2) limits. This is in accordance with the isotropic arrangement of the polymer chains in these films. The equilibrium swelling levels increased with increasing pH, reflecting the anionic nature of PAA polyelectrolyte.

As CF-2 was cross-linked at a lower temperature (by 6 °C) than CF-1, less cross-linking is expected. This implies

Table 2
Heating conditions and mass loss after 2-week water immersion

	Cast film		ES membrane		
	CF-1	CF-2	ES-1	ES-2	ES-3
Heating temperature (°C)	143	135	144	138	137
Heating time (min)	8	8	5	5	8
Mass loss (%)	4.5	15.7	8.6	17.7	7.2

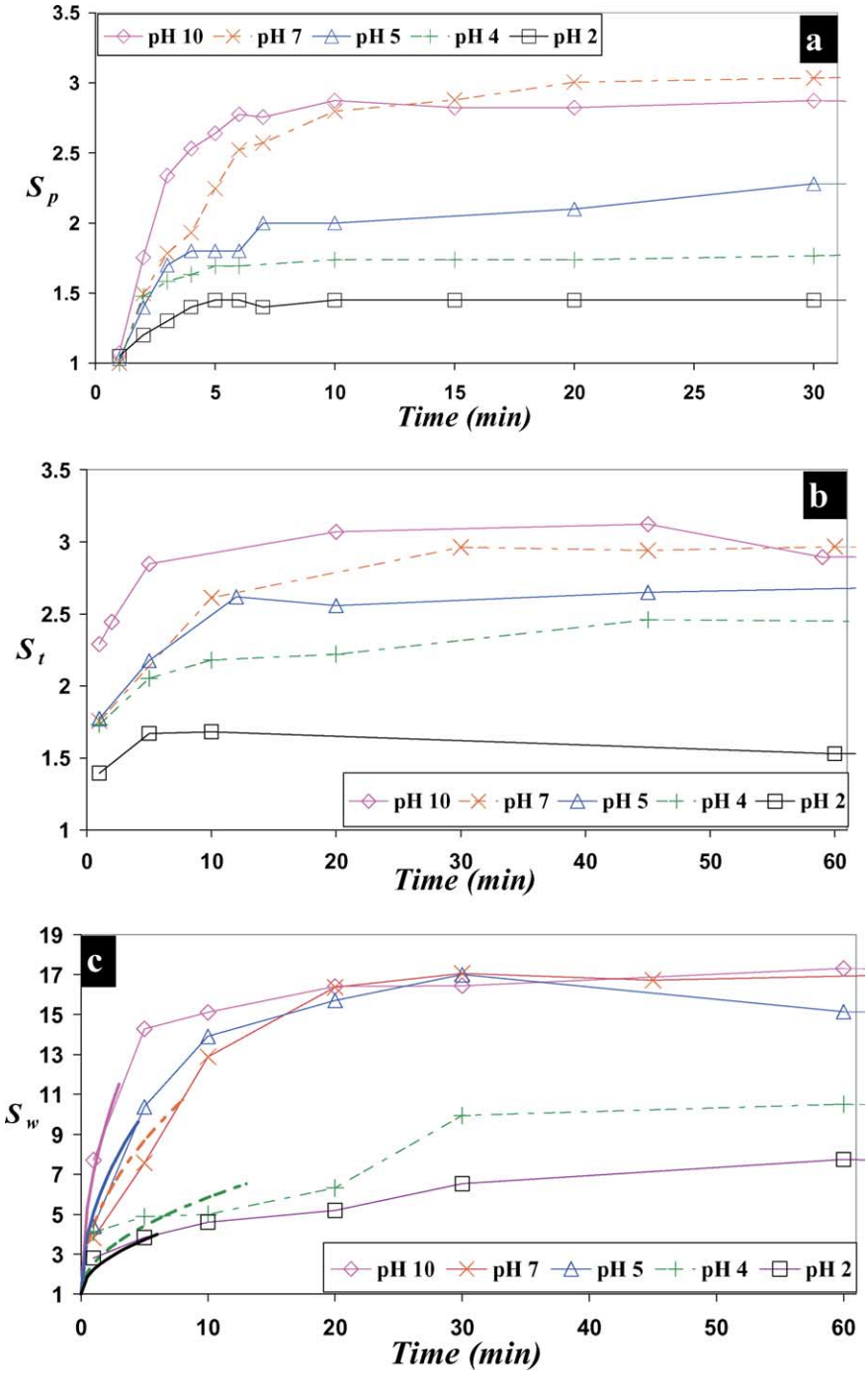

Fig. 1. Swelling behavior of cast film CF-1: (a) planar expansion S_p; (b) thickness expansion S_t; (c) mass swelling S_w. The fitting curves in (c) are indicated with thicker lines.

that CF-2 has longer chain segments between cross-link junctions. Swelling ratio in polymer networks has been described by the following equation [6]:

$$q^{5/3} = \frac{(1/2 - \chi)2M_c}{V_1\rho_0\nu^{2/3}(1 - 3M_c/M_n)}$$

where q is the volume swelling ratio, χ is the interaction parameter between polymer and solvent, V_1 is the molar volume of the liquid, ρ_0 is the density of the dry polymer, ν is the volume fraction of the polymer after cross-linking, M_c is the molecular weight of the segment between cross-linking junctions, M_n is the molecular weight of polymer chain before cross-linking. Generally, the larger the M_c, the higher the swelling ratio, so the less cross-linked film CF-2 should have a higher swelling extent than CF-1 as observed. The q value can be estimated as $S_{p,e}^2 S_{t,e}$. The q and S_w for

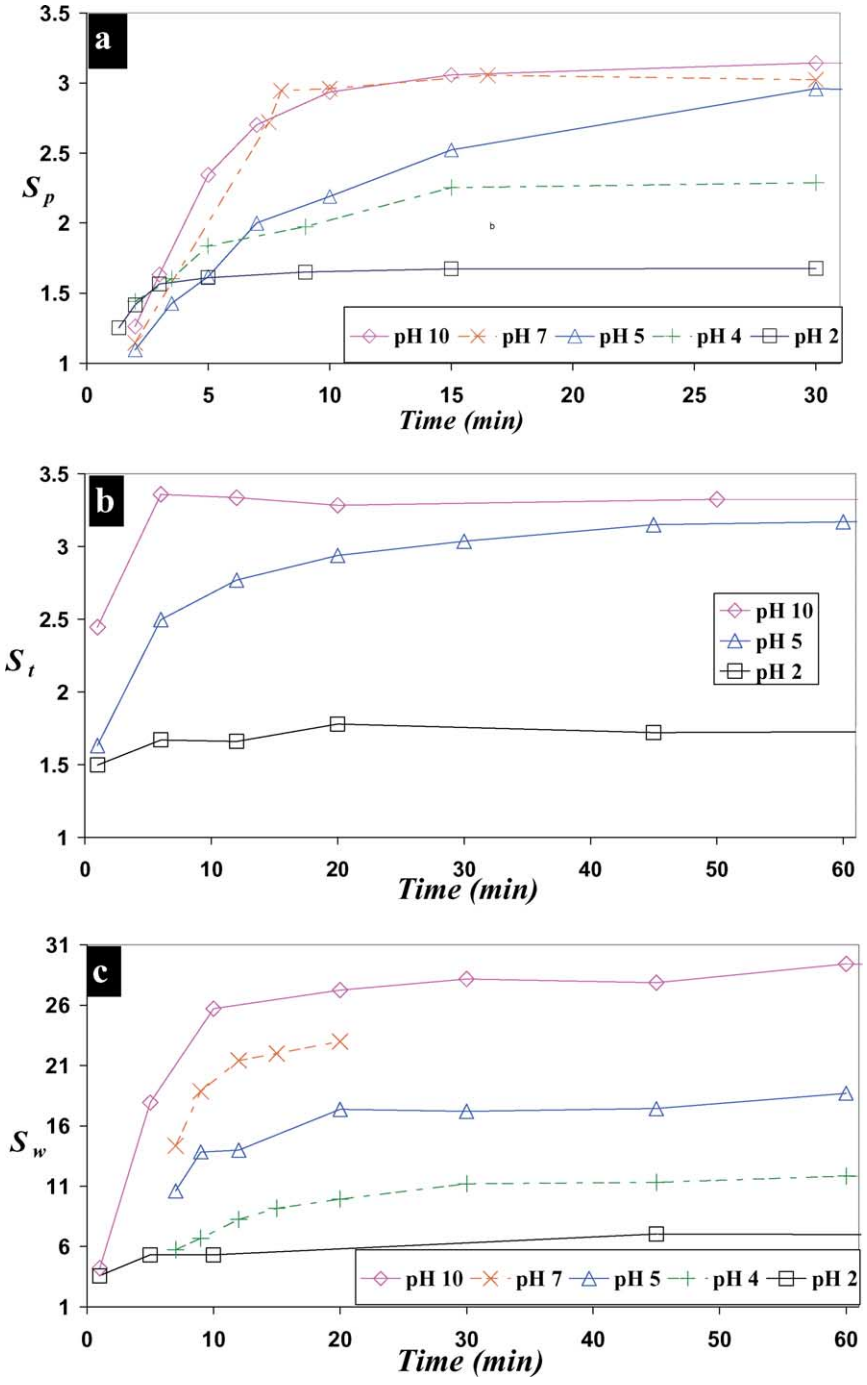

Fig. 2. Swelling behavior of cast film CF-2: (a) planar expansion S_p; (b) thickness expansion S_t; (c) mass swelling S_w.

film CF-2 are ~1.2 and ~1.6 times of those for CF-1, respectively. Considering the experimental error, the volume and weight increases are comparable. This agrees with general expectation.

The gradual upward swelling curve before equilibrium corresponds to the diffusion of water molecules and salt ions into the gel. Solving the Fick's second law of diffusion in one dimension with certain boundary conditions leads to an expression that relates the mass of the liquid absorbed or released, M, with time, t [19]

$$\frac{M_t}{M_\infty} = kt^n \tag{2}$$

where the subscript ∞ represents infinite time, and k is a constant related to both the diffusion constant and sample's characteristic length (thickness or diameter, etc). In Fickian diffusion, or case I diffusion, $n=0.5$. In cases, where $0.5<n<1$, they are normally referred to as anomalous diffusion. For the case II diffusion, where $n=1$, it is generally believed that the solvent diffusion and the polymer matrix relaxation

are coupled. The coupling effect also has contribution in anomalous diffusions. The initial mass swelling data of CF-1 (Fig. 1(c)) was fitted to Eq. (2), with $(S_w-1)/(S_{w,e}-1)$ replacing M_t/M_∞. Obviously, the data do not exhibit case II ($n=1$) behavior, since they do not form a straight line. The fitting with $n=0.5$ (shown as thick lines as opposed to the thin interpolating lines in Fig. 1(c)) generally overlap experiment data. The initial swelling data in Fig. 1(c), (for most pH values) also fit well with $n>0.5$, e.g. 0.6 or 0.7. These results suggest a slightly non-Fickian anomalous diffusion. Our data did not show the peculiar swelling behavior with overshooting [20] or sigmoid [21] shapes reported before.

Film thickness showed strong influence on its swelling behavior. The CF-1 (Fig. 1) and CF-2 (Fig. 2) films were 0.12–0.25 mm in thickness. A much thicker (0.6–0.7 mm) film was also prepared and cross-linked under the same condition as CF-2 for comparison. This thicker film took 10 time longer to reach a much lower equilibrium $S_{w,e}$ (Fig. 3). The response time of a gel has been given as $x^2/2D$ [22,23], where x is the characteristic diffusion distance and D is the diffusion coefficient. The one-magnitude longer time taken to reach S_w equilibrium for a film 3–4 times thicker confirms that the second-power dependence of diffusion time on thickness also applies here. The theoretical diffusion relationship when applied on ultra-fine fibers in fibrous membrane should predict a remarkably fast response.

3.2. Fibrous membrane

The fibrous membranes composed of ultra-fine fibers with diameters of 100–500 nm and much larger interconnected inter-fiber spaces (Fig. 4). The porosity of these fibrous membranes was estimated by the absorption of hexadecane, a low surface tension and low viscosity liquid. The porosities of all three membranes were found to be around $40\pm5\%$. By default, cast film and ES membrane were 0.12–0.25 mm and 0.3–0.5 mm thick, respectively. Based on the porosity and thickness of the films and fibrous membranes, their weight should be comparable at similar planar dimensions as observed. Using the mass and size (thickness and planar dimension) measured, the densities of films and fibrous membranes were calculated to be 1.1 ± 0.1 and 0.68 ± 0.1 g/cm^3, respectively. The fibrous membranes were about ~60% as dense as the films, consistent with the estimated porosity.

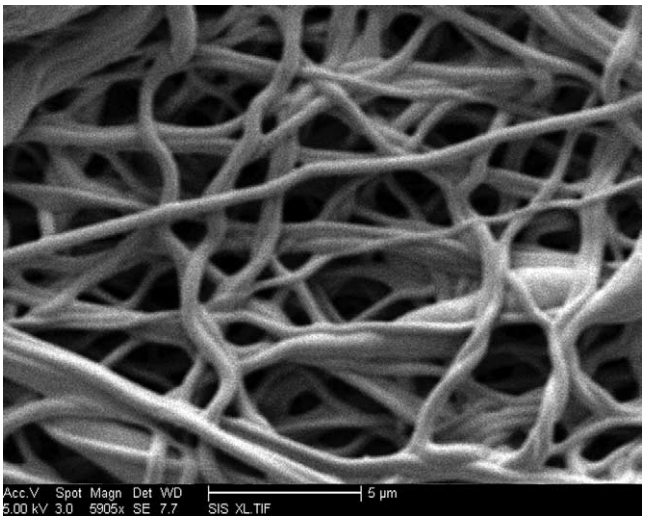

Fig. 4. SEM image of thermally cross-linked fibrous membrane ES-1.

For the fibrous membrane ES-1 (cross-linked at 144 °C for 5 min), the planar swelling equilibrium was reached within 1 min in pH 2 buffer, and ~10 min in other buffers (Fig. 5(a)). In contrast, swelling in thickness (Fig. 5(b)) reached equilibrium within a minute in both pH 10 and 2 buffers, but took much longer time (~40 min) in the middle pH range. The mass swelling data of ES-1 were also fitted with Eq. (2) using n of 0.5 as shown in Fig. 5(c). The fitting of this fibrous membrane showed a slightly non-Fickian anomalous behavior similar to the film CF-1.

In view of the diffusion time dependence of x^2/D mentioned above, membranes containing ultra-fine fibers are expected to reach swelling equilibrium much faster than

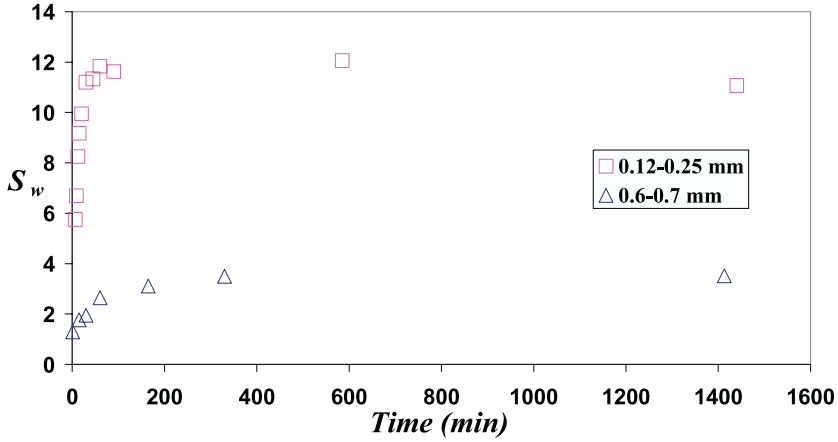

Fig. 3. Thickness influence on mass swelling of cast film CF-2 in pH 4 buffer.

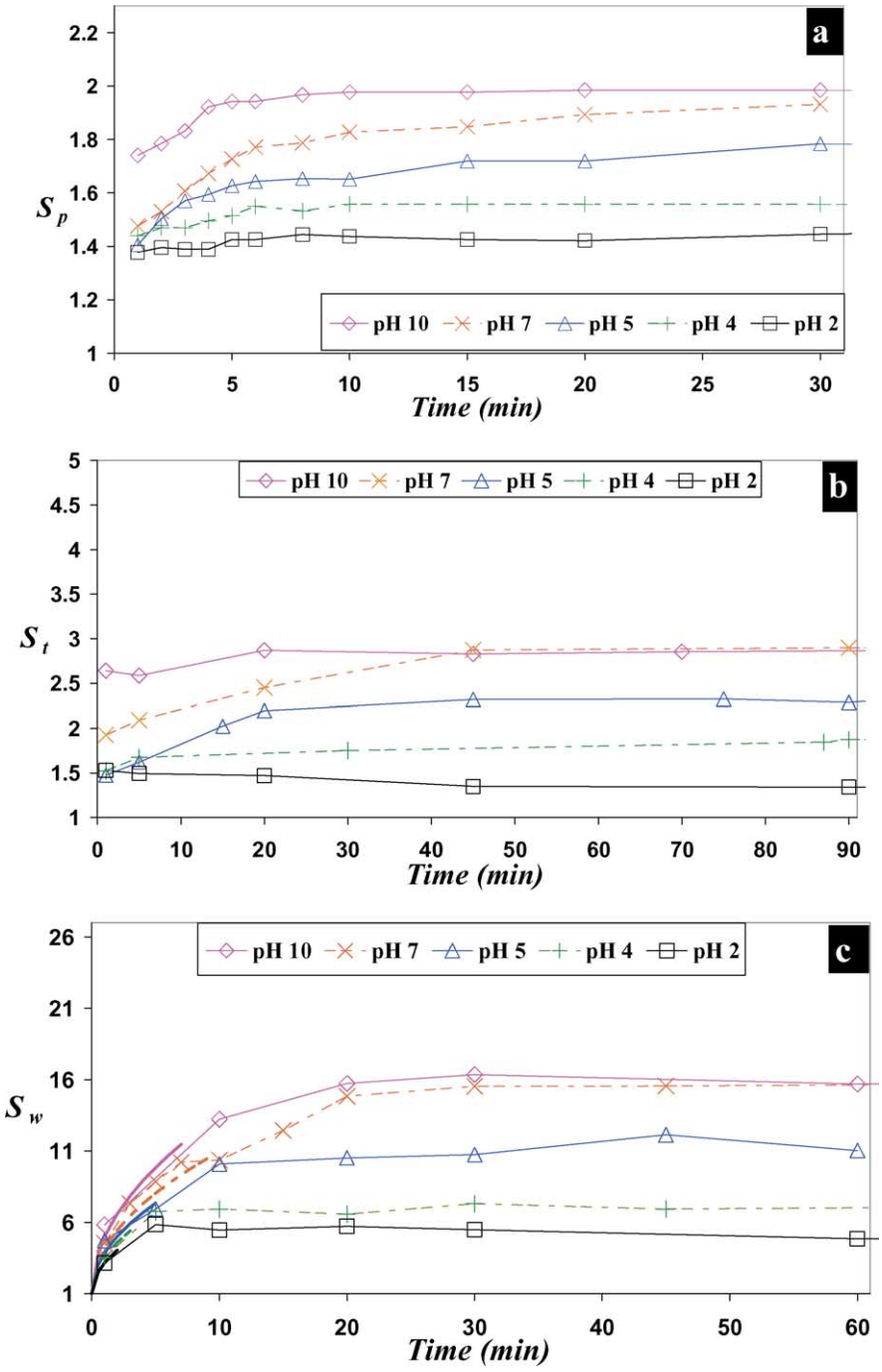

Fig. 5. Swelling behavior of fibrous membrane ES-1: (a) planar expansion S_p; (b) thickness expansion S_t; (c) mass swelling S_w. The fitting curves in (c) are indicated with thicker lines.

monolithic film. However, the data above suggest the inter-fiber pore structure within the membrane has significant influence on the overall uptake of liquid as well as the swelling of fibers located internally in the membranes. For individual fibers in contact with a liquid reservoir, the diffusion time dependence of x^2/D should still hold. So upon immersion of the fibrous membrane in a buffer, the ultra-fine fibers on membrane surface should be able to instantly absorb the liquid and expand to consume much of the inter-fiber space in their vicinity. The fibers located further away from the surface of the membrane also undergo the same process once the inter-fiber pores at their neighbor are filled with the liquid. It is the filling of these internal pores of the membranes that influence the swelling of fibers located there. Instantaneous swelling of surface fibers is thought to reduce the surface pore sizes. Hence behind the liquid diffusion front a distribution of the pore sizes of inter-fiber space is formed, i.e. larger pore sizes among the internal dry

fibers than those among swollen surface fibers. The smaller inter-fiber pore size enhances the capillary pressure driving liquid wicking, but it also significantly reduce the quantity of liquid to be transported into the membrane. So the reduced inter-fiber pore sizes resulted from fiber swelling on the membrane surfaces hamper the transportation of the liquid inward to the larger internal pores in the fibrous membranes. Thereby the apparent mass swelling behavior of fibrous membrane differentiated not much from that of the film, and an extraordinarily fast mass uptake was not observed for fibrous membrane. The detailed mechanisms may deserve the modeling work with consideration of the rates for inter-fiber wicking, intra-fiber diffusion and fiber swelling.

Fibrous membrane ES-2 was cross-linked at lower temperature (138 °C) than ES-1 (144 °C) for the same time length (5 min). The equilibrium swelling in planar dimension, thickness and mass of ES-2 (Fig. 6) is clearly higher than ES-1 (Fig. 5) and is consistent with the less cross-linked structure in ES-2. At pH 10, the equilibrium volume expansion of ES-2 estimated from the planar and thickness expansion values is ~1.8 times of ES-1 (mainly from the contribution of $S_{t,e}$ increase), and is comparable to the ratio of $S_{w,e}$, which is ~1.6.

Fibrous membrane ES-3 was processed at a lower temperature (137 °C) than ES-1, but longer by 3 min. Its planar (Fig. 7(a)) and mass (Fig. 7(c)) swelling behavior were comparable to those of ES-1, but its $S_{t,e}$ (Fig. 7(b)) at high pH (pH 10) is evidently lower than that of ES-1 (Fig. 5(b)). These observations suggest that ES-3 membrane has an extent of cross-linking similar to or higher than that of ES-1. Previous research [18] showed that the cross-linking extent and consequently swelling degree of thermal cross-linked PVA/PAA (4 w/w PVA/PAA) films (0.1–0.2 mm) depended mainly on temperature, while the length of heating time had only small influence. Our observation on these fibrous membranes indicated that the length of heating affect comparably to, if not more than, temperature under our heating conditions and compositions. Although the heating conditions are close between CF-2 film (Fig. 2) and ES-3 fibrous membrane (Fig. 7), both dimensional and mass swelling of the film exceeded those of the fibrous membrane. This could be associated with a less cross-linked structure due to lower thermal diffusion in the thicker and denser monolithic film.

The planar expansion of fibrous membranes occurred instantaneously (Figs. 5(a), 6(a) and 7(a)) and did not exhibit the initial time lags observed with the films (Figs. 1(a) and 2(a)). For monolithic film, the observable planar expansion occurs only after the slow diffusion of liquid through the much longer distance in the thickness direction. For fibrous membrane, albeit their apparent mass swelling pattern comparable to that of monolithic film, the outside layers expand in planar direction quickly, followed by the swelling and shifting of inner fiber layers. This could be the reason for the absence of the initial lag in planar expansion. However, the planar expansion of fibrous membranes was still affected when liquid diffusion was reduced by fiber swelling as discussed above. For the less cross-linked ES-2, relatively higher extent swelling of the fibers is expected, and the reduced liquid diffusion caused its initial planar expansion (Fig. 6(a)) to be even lower than those of the more cross-linked ES-1 (Fig. 5(a)) and ES-3 (Fig. 7(a)).

The most intriguing observation is the considerably higher equilibrium expansion in thickness than in the planar direction for all three fibrous membranes. This character is most obvious for less cross-linked ES-2 (Fig. 6(a) compared with Fig. 6(b)). Even for the relatively highly cross-linked ES-1, $S_{p,e}$ (Fig. 5(a)) was ~2 but $S_{t,e}$ was ~3 at pH 10 (Fig. 5(b)). This peculiar asymmetric dimensional swelling behavior is explicable with the asymmetric distribution of the fibers in the planar and thickness directions (Fig. 4). In the planar directions, fibers are randomly distributed in layers, in which the interfiber spaces are much larger relative to those between layers and can be envisaged to be many largely planar plate-like spaces. Upon absorbing the liquid, the fibers can swell into these relatively voluminous interfiber spaces, therefore, leading to less expansion in the planar directions, i.e. lower contribution to $S_{p,e}$. Therefore, the $S_{p,e}$ of the whole fibrous membrane is smaller than that of film. Whereas along the thickness direction, because fibers are laid on layer by layer tightly during electrospinning, there are numerous contact points between fibers in neighbor layers. Swelling of individual fibers at these crossover contact points cannot be accommodated by inter-fiber spaces and result in a $S_{t,e}$ much higher than $S_{p,e}$.

Another possible explanation for the asymmetric swelling is the preferential orientation of polymer chains along fiber axis caused by the strong electrical field during electrospinning. Raman spectra studies indicated that electrospinning can convert the crystalline structure of Nylon 6 from α-form in bulk samples to γ-form, but no effect of electrospinning was observed for Nylon 12, which has only one preferred conformation [24]. Thus far very little is known about the alteration of chain configuration by electrospinning or the existence of long-range chain orientation in electrospun fibers. Therefore, the mesoscopic asymmetric arrangement of electrospun fibers is regarded as the dominant factor for the asymmetric dimensional swelling of fibrous membranes.

For fibrous membranes, planar expansion (S_p) reaches equilibrium (in ~5 min) ahead of thickness (S_t) and mass (S_w) expansion (in ~20 min or longer) especially at intermediate pH values. This implicates that the fiber shifting accompanying fiber expansion causes changes on inter-fiber pore structure such as total porosity, pore volume, pore connectivity, and the adjustment process takes longer time to settle than planar expansion. This is also in agreement with the above justification for the comparable mass swelling behavior of monolithic film and fibrous membrane.

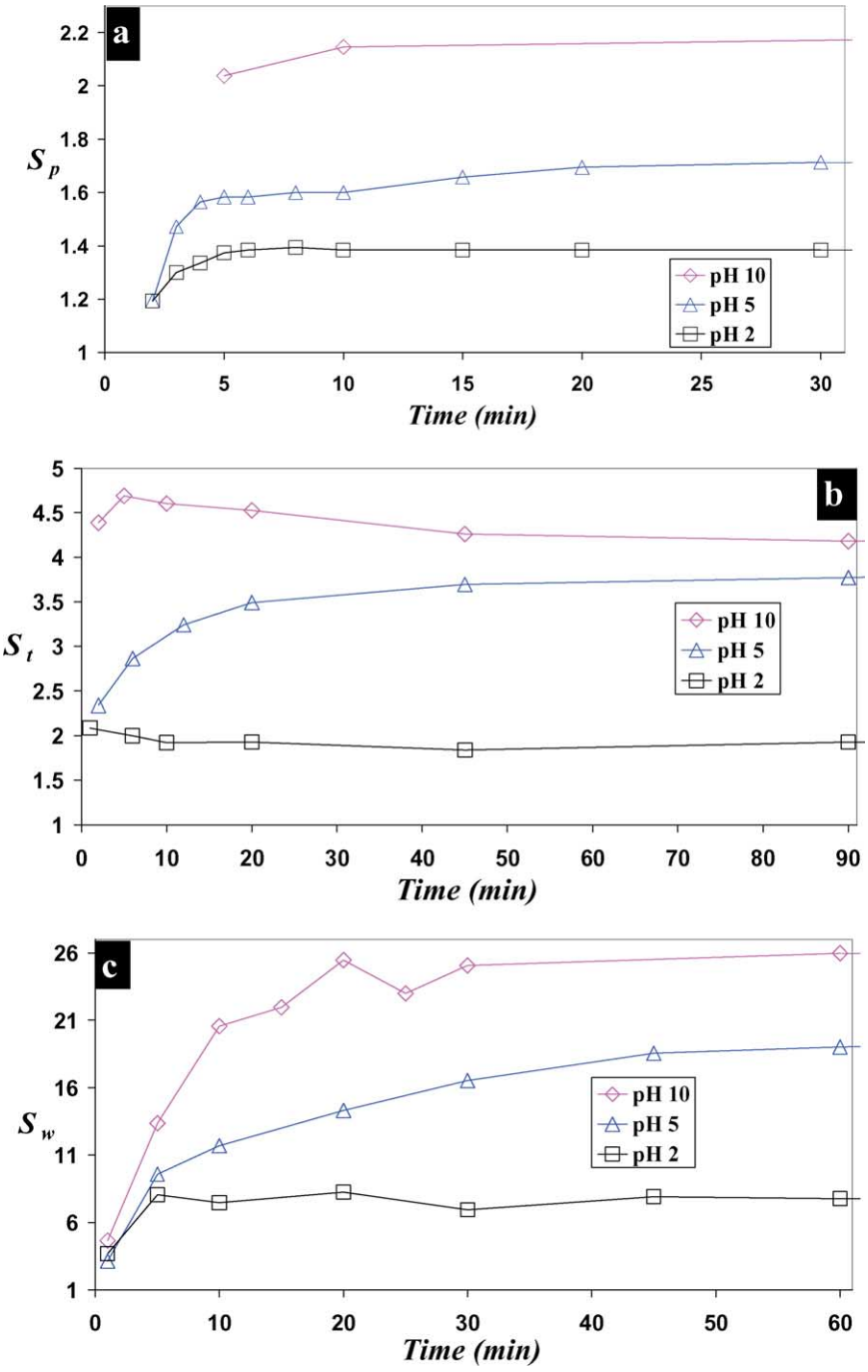

Fig. 6. Swelling behavior of fibrous membrane ES-2: (a) planar expansion S_p; (b) thickness expansion S_t; (c) mass swelling S_w.

We also studied the influence of sample thickness on the swelling behavior of fibrous membrane by comparing the mass swelling behavior of ES-1 to a thinner fibrous membrane processed at the same thermal cross-linking condition (Fig. 8). The default thickness of fibrous membrane was 0.3–0.5 mm. Thinner (0.1–0.15 mm) membrane has almost the same $S_{w,e}$, nevertheless it reaches S_w equilibrium much faster (<1 min). For this thin fibrous membrane, liquid may have diffused through the sample before swollen fibers fill up interfiber spaces to impede the adsorption as discussed above.

3.3. General discussions

The monolithic films were rigid, translucent and turned light yellow upon heat-induced cross-linking. These films became completely transparent, elastic gels in aqueous buffers after several minutes. The fibrous membrane exhibited much different characteristics at different experiment stages. The as-spun fibrous membranes were white and flexible similar to tissue paper. After thermal cross-linking, it shrank and became rigid and slightly

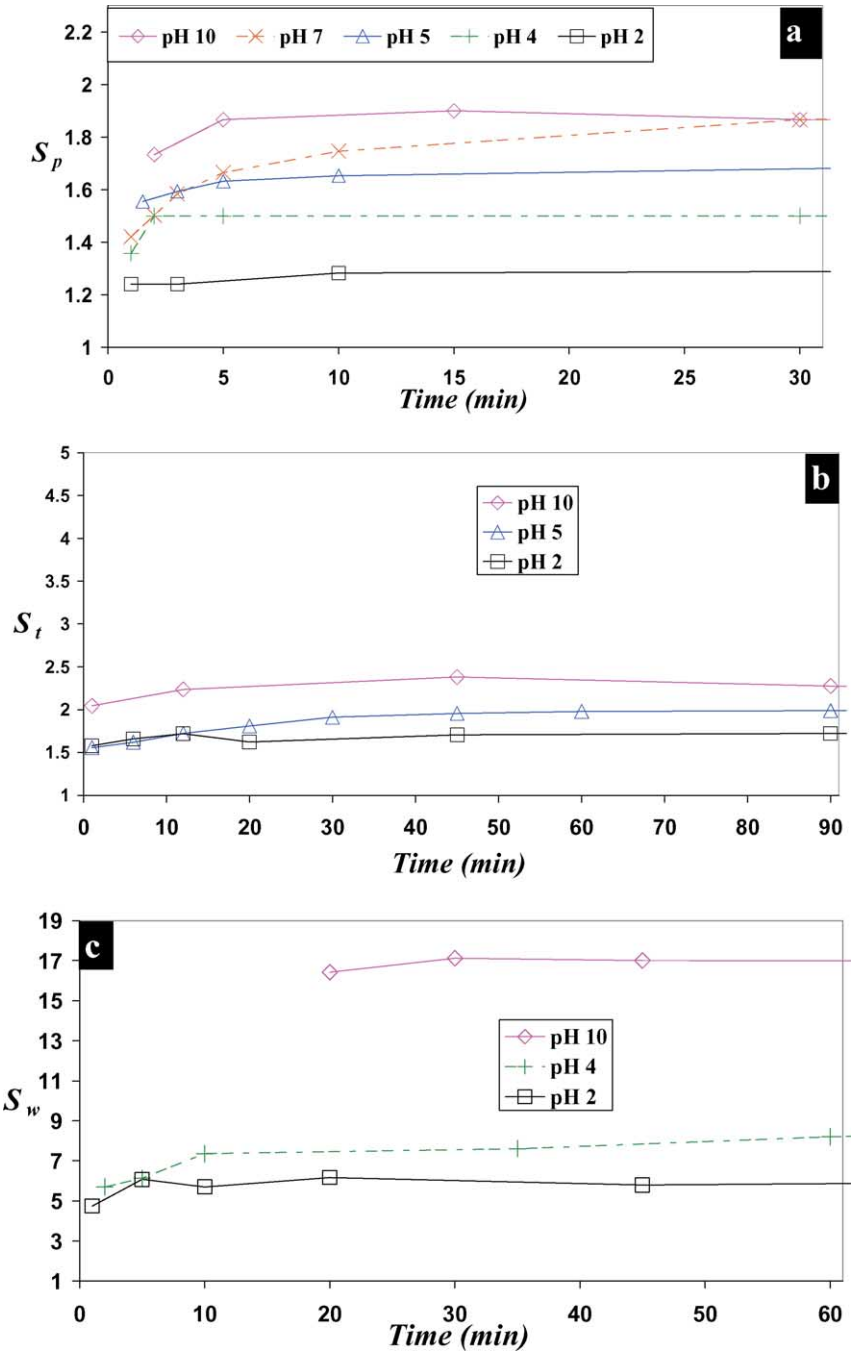

Fig. 7. Swelling behavior of fibrous membrane ES-3: (a) planar expansion S_p; (b) thickness expansion S_t; (c) mass swelling S_w.

yellow, appeared and felt like a wood flake. The fibrous membrane became gel-like and nearly translucent in aqueous solutions.

Swollen monolithic films were very easy to break under distortion, especially at higher swelling extent (i.e. at high pH condition), whereas swollen fibrous membranes behaved like a rubber and could always retain good shape without huge distortion force. The porous structure of the fibrous membranes makes them flexible and withstanding distortion and external forces better. For fibrous membranes, cross-linking may occur not only within fibers as in the films, but also in some extent at some inter-fiber crossover contacting points, which helps to maintain integrity.

Some fully swollen (i.e. after reaching equilibrium) samples were centrifuged for 6 min at 3000 rpm (i.e. ω, 314 rad/s) and the centripetal acceleration ($\omega^2 r$) is 1207g (g: gravity; 9.8 m/s^2) with a 12-cm radius. The amount of absorbed liquid remained after centrifuge treatment is listed in Table 3. Sample dimensions had no significant changes in the whole process. If centrifuged-off liquid are related simply to the fraction not wiped away on sample surface, then the residual liquid should remain almost constant, but

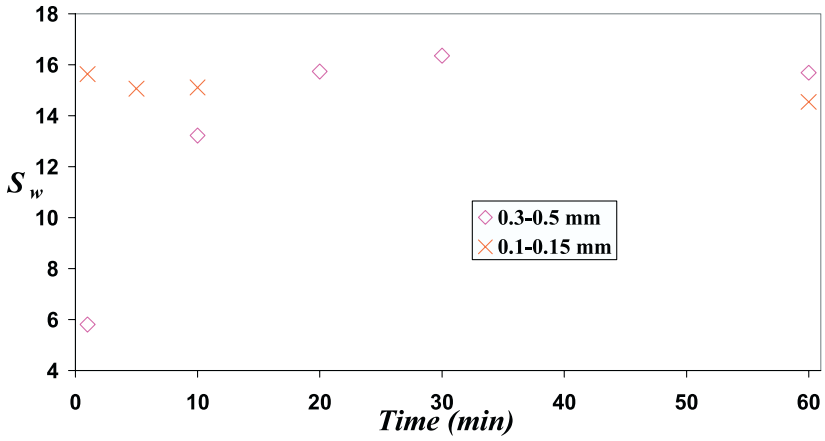

Fig. 8. Thickness influence on mass swelling of fibrous membrane ES-1 in pH 10 buffer.

this was not the case for either film or fibrous membrane. For films, there is a transition around the pK_a of acrylic acid, above which the percentage of remained liquid is almost constant. For fibrous membranes, in contrast, the residual liquid increased steadily with increasing pH. This indicates that fibers become more swollen and closely packed with increasing pH if centrifuged-off liquid is mainly related with fraction at inter-fiber spaces. After samples were put back to buffer for >17 h, the centrifuge experiments were repeated, and comparable data were obtained.

When placing the centrifuged samples to the buffer, fibrous membranes returned to pre-centrifuge $S_{w,e}$ in less than 14 s, much faster than the dry membranes. For films the time to reach $S_{w,e}$ for centrifuged samples is commensurate with that for dry samples. The results were independent of pH values. Therefore, the time to reach $S_{w,e}$ for centrifuged fibrous membranes is evidently shorter than those for centrifuged films and dry membranes. This is in stark contrast to the comparable mass swelling behavior for dry membranes and films as presented above. This is understandable since, as discussed above the mass uptake of the dry membrane is barricaded with a slow process of structure adjustment, whilst the reswelling of centrifuged membrane only involves the inter-fiber wicking as the fibers are already swollen as hydrophilic gels. Moreover, solvent can reduce the glass transition of polymer matrix, and the effect still largely holds in centrifuged sample. This allows an easier rearrangement of polymer chains to accept liquid before returning to equilibrium. The finding shows that fibrous membranes in the swollen state may serve better than at dry state in applications that require instantaneous liquid uptake.

Table 3
Percentage of liquid remained in swollen samples after centrifugation

pH	2	5	10
ES-1	67	78	84
CF-1	66	90	88
CF-2	63	–	85

The values were calculated as $(W_c - W_d)/(W_e - W_d)$, where W_c, W_e, and W_d, are the weights of centrifuged, mass swelling equilibrated, and dry samples, respectively. The standard deviation of the data is ~ 3.

4. Conclusions

Monolithic films and fibrous membranes were prepared from aqueous mixtures of PVA/PAA (3.5 COOH/OH) by solvent casting and electrospinning, respectively. The samples were rendered water-insoluble by heat-induced esterification, and their dimensional (planar and thickness) and mass-swelling behavior were measured in buffers ranging from pH 2–10. Lower extents of swelling at higher temperature and longer heating time (5 or 8 min between 135 and 144 °C) indicated higher esterification. The extent of cross-linking were similarly affected by the length and temperature of heating.

The equilibrium swelling of both films and fibrous membranes increased with increasing pH. For the monolithic films, equilibrium swelling extents in the planar and thickness directions were comparable at each pH level, in accordance with the isotropic polymer chain arrangement. In contrast, the fibrous membranes exhibited significantly higher equilibrium swelling in the thickness than in the planar direction over the entire pH range. This peculiar asymmetric swelling behavior was associated with the asymmetric distribution of fibers in planar and thickness directions, resulted from the layer-by-layer build-up of electrospinning. Upon absorbing liquid, fiber swelling reduced interfiber spaces along the planar directions, reducing their contribution to the planar expansion of the entire membrane. In the thickness direction, swelling of the membrane were more than additive of individual swollen fibers to render the total expansion higher than that on planar direction.

The initial mass swelling behavior of all samples showed slightly non-Fickian anomalous behavior. For fibrous membranes, swelling in the thickness direction and mass

uptake lasted longer after planar expansion had stopped. These results testify that inter-fiber space is filled up by swollen fibers, and the process gradually develops from surface inwards. The planar expansion of the fibrous membranes occurred immediately upon exposure to the buffers, without the time lags observed on the films. For the less cross-linked ES-2, higher swelling of fibers near the membrane surfaces may reduce the inter-fiber spaces more rapidly, slowing the initial planar swelling more than those of the more cross-linked ES-1 and ES-3.

For monolithic films, the time to reach equilibrium mass swelling for centrifuged samples was commensurate with that for dry samples. For fibrous membranes, the centrifuged samples reached equilibrium mass swelling remarkably faster than original dry ones. Furthermore, the fibrous gel membranes had much better shape and strength retention, making them more versatile and superior to cast-film gels as practically useful electro- or pH-activation assembles.

Acknowledgements

The authors would like to thank Mr Lei Li for his very helpful discussions and the National Textile Center (Project M04-CD01s) for partial support of this project.

References

[1] Osada Y, Gong JP. Adv Mater 1998;10:827.
[2] Tanaka T, Fillmore DJ, Sun ST, Nishio I, Swislow G, Shah A. Phys Rev Lett 1980;45:1636.
[3] Tanaka T, Nishio I, Sun ST, Ueno-Nishio S. Science 1982;218:467.
[4] Hamlen RP, Kent CE, Shafer SN. Nature 1965;206:1149.
[5] Schreyer HB, Gebhart N, Kim KJ, Shahinpoor M. Biomacromolecules 2000;1:642.
[6] Buchholz FL, Graham AT, editors. Modern superabsorbent polymer technology. New York: Willey; 1998.
[7] (a) Lee YM, Kim SH, Cho CS. J Appl Polym Sci 1996;62:301.
(b) Bromberg L, Temchenko M, Moeser GD, Hatton T. Langmuir 2004;20:5683.
[8] (a) Argade AB, Peppas NA. J Appl Polym Sci 1998;70:817.
(b) Kim J, Serpe MJ, Lyon LA. J Am Chem Soc 2004;126:9512.
[9] Kuhn W, Hargitay B, Katchasky A, Eisenberg H. Nature 1950;165: 514.
[10] (a) De Rossi D, Chiarelli P, Buzzigoli G, Domenici C. Trans Am Soc Artif Intern Organs 1986;32:157. (b) As quoted in Ref. 10(a) Kuhn W, Hargitay B. Elektrochem 1951;55:490.
[11] Shahinpoor M. Electrochim Acta 2003;48:2343.
[12] (a) Kim SY, Shin HS, Lee YM, Jeon CN. J Appl Polym Sci 1999;73: 1675.
(b) Fei J, Zhang Z, Gu L. Polym Int 2002;51:502.
[13] Li D, Xia Y. Adv Mater 2004;16:1151.
[14] Chen H, Hsieh Y-L. J Polym Sci Part A: Polym Chem 2004;42:6331.
[15] Li L, Hsieh Y-L. Am Chem Soc Polym Mater Sci Eng 2004;90:639.
[16] McGaugh MC, Kottle S. J Polym Sci Polym Lett 1967;5:817.
[17] Eisengberg A, Yokoyama T, Sambalido E. J Polym Sci: Part A1 1969; 7:1717.
[18] Arndt KF, Richter A, Ludwig S, Zimmermann J, Kressler J, Kuckling D, et al. Acta Polym 1999;50:383.
[19] (a) Ritger PL, Peppas NA. J Controlled Release 1987;5:23.
(b) Ritger PL, Peppas NA. J Controlled Release 1987;5:37.
[20] Diez-Pena E, Quijada-Garrido I, Barrales-Rienda JM. Macromolecules 2003;36:2475.
[21] Diez-Pena E, Quijada-Garrido I, Barrales-Rienda JM. Macromolecules 2002;35:8882.
[22] Calvert P. In: Bar-Cohen Y, editor. Electroactive polymer (EAP) actuators as artificial muscles. Washington, DC: The Society of Photo-optical Instrumentation Engineers; 2001 [Chapter 5].
[23] Tanaka T, Fillmore DJ. J Chem Phys 1979;70:1214.
[24] Stephens JS, Chase DB, Rabolt JF. Macromolecules 2004;37:877.